

AD-A130 372

FORCED VIBRATION OF TIMOSHENKO BEAMS MADE OF
MULTIMODULAR MATERIALS..(U) OKLAHOMA UNIV NORMAN SCHOOL
OF AEROSPACE MECHANICAL AND NUCLE..
F GORDANINEJAD ET AL. JUN 83 OU-AMNE-83-2

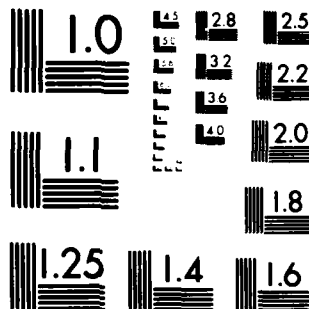
1/)

UNCLASSIFIED

F/G 11/10

NL

END
DATE
FILMED
8 83
DTIC



MICROCOPY RESOLUTION TEST CHART
NATIONAL BUREAU OF STANDARDS 1963-A

12

AD A130572

Department of the Navy
OFFICE OF NAVAL RESEARCH
Mechanics Division
Arlington, Virginia 22217

Contract N00014-78-C-0647
Project NR 064-609
Technical Report No. 33

Report OU-AMNE-83-2

FORCED VIBRATION OF TIMOSHENKO BEAMS MADE
OF MULTIMODULAR MATERIALS

by

F. Gordaninejad and C.W. Bert

June 1983

DTIC
SELECTED
JUL 12 1983
A

DTIC FILE COPY

School of Aerospace, Mechanical and Nuclear Engineering
The University of Oklahoma
Norman, Oklahoma 73019

Approved for public release; distribution unlimited

83 07 12 018

FORCED VIBRATION OF TIMOSHENKO BEAMS MADE
OF MULTIMODULAR MATERIALS¹

C.W. Bert
Perkinson Professor of Engineering

F. Gordaninejad
Graduate Research Assistant

School of Aerospace, Mechanical and Nuclear Engineering
The University of Oklahoma
Norman, Oklahoma



Accession For	
NTIS GRA&I	<input checked="" type="checkbox"/>
DTIC TAB	<input type="checkbox"/>
Unannounced	<input type="checkbox"/>
Justification	
By	
Distribution/	
Availability Codes	
Dist	Avail and/or Special
A	

¹ The research reported upon here was supported by the Office of Naval Research, Mechanics Division. The encouragement of Dr. Nicholas Basdekas is sincerely appreciated.

1 INTRODUCTION

Many materials have different elastic behavior in tension and compression. A few examples of such materials are concrete, rock, tire-cord rubber, and soft biological tissues. As early as 1864, St. Venant [1] recognized this behavior by analyzing the pure bending behavior of a beam having different stress-strain curves in tension and compression. Timoshenko [2] originated the concept of bi-modulus (or bimodular) materials in 1941 by considering the flexural stresses in such a material undergoing pure bending. Ambartsumyan [3] in 1965 renewed interest in the analysis of bimodular materials, i.e., materials having different moduli in tension and compression. Since then, there have been numerous investigations on the static behavior of bimodular beams; these were surveyed by Tran and Bert [4]. Recently, Bert and Gordaninejad [5] studied bending of thick beams of "multimodular" materials.

Only a few studies have been made on vibration of bimodular beams. Recently, Bert and Tran [6] worked on transient response of thick beams of bimodular materials.

The present paper deals with the forced vibration of beams made of "multimodular" materials. The transfer-matrix method [7], which computationally is very efficient, is applied. Also, the beam is modeled as a Timoshenko beam, i.e., both transverse shear deformation and rotatory inertia are considered.

2 MODELING OF THE STRESS-STRAIN CURVE

The nonlinearity of the stress-strain curve is one of the main difficulties arising in structures undergoing even moderate deflections. Piecewise linearization of the stress-strain relation has been applied to overcome this problem. Durban and Baruch [8] used a floating piecewise linear approximation to construct the two "best" straight lines approximating the Ramberg-Osgood stress-strain relation [9]. Bert and Kumar [10] recently presented experimental stress-strain curves

for unidirectional cord-rubber materials and expressed the curves in Ludwik power-law form with different coefficients and exponents in tension and compression.

In the present work, a stress-strain curve for aramid-rubber taken from [10] has been linearly approximated by four segments (two segments in tension and two segments in compression; see Fig. 1). For choosing the "best" two straight lines, the area between two fitting lines and the experimental curve in each portion has been minimized. To find comparable moduli for the bimodular case, one has to minimize the area between two straight lines and the experimental curve. Finally, for the "unimodular" case, the "best" single straight line is used (see Appendix A).

3 CLOSED-FORM SOLUTION

Consider a solid rectangular-cross-section beam of thickness h and length l . The beam coordinates are taken such that the xy -plane coincides with the mid-plane of the beam and the z -axis is measured positive downward. For a four-segment approximation of the normal stress-strain curve, considering the general case (i.e., when $-h/2 < a_c$, $a_t < h/2$), the following stress field has been considered for the case of convex bending (see Figs. 1 and 2).

$$\sigma_x \equiv \begin{cases} E_1^c \epsilon_1^c + E_2^c (\epsilon_x - \epsilon_1^c) & -h/2 < z < a_c \\ E_1^c \epsilon_x & a_c < z < z_n \\ E_1^t \epsilon_x & z_n < z < a_t \\ E_1^t \epsilon_1^t + E_2^t (\epsilon_x - \epsilon_1^t) & a_t < z < h/2 \end{cases} \quad (1)$$

$$\tau_{xz} = G \gamma_{xz} \quad (2)$$

where $E_1^c, E_2^c, E_1^t, E_2^t, G, \epsilon_1^c$, and ϵ_1^t are material constants, σ_x is the axial normal stress, ϵ_x is the axial normal strain, γ_{xz} is the transverse shear strain, τ_{xz} is the transverse shear stress, and z_n is the location of the neutral surface.

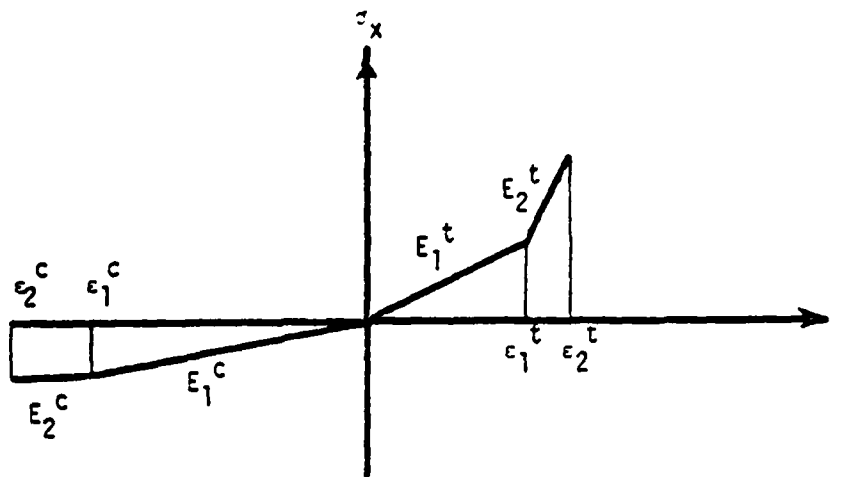


Fig. 1 Multimodular model.

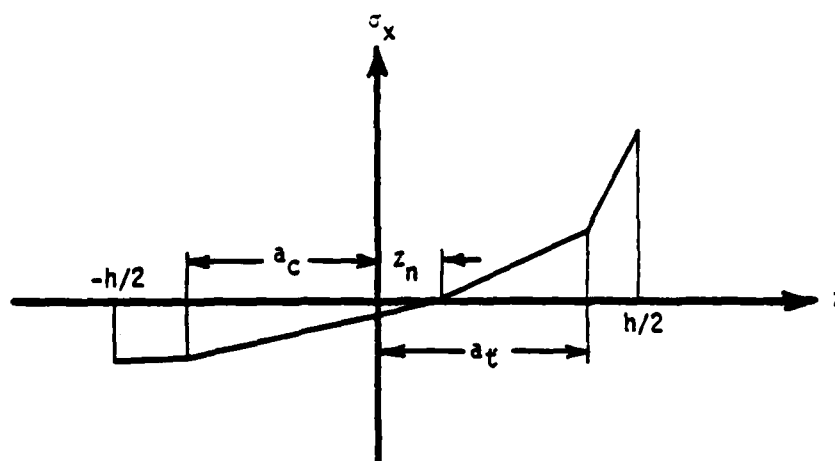


Fig. 2 Stress Distribution of a Multimodular Beam for Convex Bending

It is noted that this material is linear elastic in shear. Comparison of Figs. 1 and 2 leads to

$$\epsilon_x = \kappa(z - z_n) \quad (3)$$

$$\epsilon_1^c = \kappa(a_c - z_n) \quad (4)$$

$$\epsilon_1^t = \kappa(a_t - z_n) \quad (5)$$

Using linear strain measure, one obtains

$$\epsilon_x = U_{,x} = u_{,x} + z\psi_{,x} \quad (6)$$

$$\gamma_{xz} = W_{,x} + U_{,z} = w_{,x} + \psi$$

Comparison of equations (3) and (6) gives

$$u_{,x} = -\kappa z_n, \quad \psi_{,x} = \kappa \quad (7)$$

Note that $()_{,x}$ denotes $\partial()/\partial x$.

Timoshenko beam theory is implemented here, by using the definitions of the normal and transverse shear stress resultants and moment, each per unit width as follows:

$$(N, Q) = \int_{-h/2}^{h/2} (\sigma_x, \tau_{xz}) dz, \quad M = \int_{-h/2}^{h/2} z \sigma_x dz \quad (8)$$

One can write the constitutive relation for a multimodular beam as

$$\begin{Bmatrix} N \\ M \\ Q \end{Bmatrix} = \begin{bmatrix} A + C_N^A & B + C_N^B & 0 \\ B + C_M^B & D + C_M^D & 0 \\ 0 & 0 & S \end{bmatrix} \begin{Bmatrix} u_{,x} \\ \psi_{,x} \\ w_{,x} + \psi \end{Bmatrix} = \begin{bmatrix} A' & B' & 0 \\ B'' & D' & 0 \\ 0 & 0 & S \end{bmatrix} \begin{Bmatrix} u_{,x} \\ \psi_{,x} \\ w_{,x} + \psi \end{Bmatrix} \quad (9)$$

where A , B , D , and S denote the respective extensional, flexural-extensional coupling, flexural, and transverse shear stiffnesses defined by

$$(A, B, D) = \int_{-h/2}^{h/2} (1, z, z^2) E_i^{(k)} dz \quad \begin{matrix} i=1,2 \\ k=t,c \end{matrix} \quad S = K^2 \int_{-h/2}^{h/2} G dz \quad (10)$$

Here, the stiffnesses C_N^A , C_N^B , C_M^B , and C_M^D are not present in unimodular or bimodular materials (see Appendix B). In equation (10), t and c denote tensile-strain and compressive-strain regions, respectively, and K^2 is the shear correction coefficient*. The general equations of motion, if z_n (neutral-surface location) is constant along the beam are

$$\begin{aligned} A'u_{,xx} + B'\psi_{,xx} &= Pu_{,tt} + R\psi_{,tt} \\ S(w_{,xx} + \psi_{,x}) &= Pw_{,tt} - q(x, t) \\ (B''u_{,xx} + D'\psi_{,xx}) - S(w_{,x} + \psi) &= Ru_{,tt} + I\psi_{,tt} \end{aligned} \quad (11)$$

where

$$(P, R, I) = \int_{-h/2}^{h/2} \rho(1, z, z^2) dz$$

and ρ is the density of material.

For guided-guided boundary condition, i.e.,

$$\begin{aligned} u(0, t) = u(l, t) = 0 \quad ; \quad \psi(0, t) = \psi(l, t) = 0 \\ Q(0, t) = Q(l, t) = 0 \end{aligned} \quad (12)$$

if

$$q(x, t) = q_0 \cos \alpha x \cos \Omega t \quad (13)$$

then the following sets of functions satisfy the equations of motion

$$\begin{aligned} u(x, t) = \bar{U} \sin \alpha x \cos \Omega t \quad ; \quad \psi(x, t) = \bar{\Psi} \sin \alpha x \cos \Omega t \\ w(x, t) = \bar{W} \cos \alpha x \cos \Omega t \end{aligned} \quad (14)$$

*In actuality, enforcement of the axial-free equilibrium equation of elasticity requires that K^2 for a multimodular beam (even a single-layer one, such as treated here) be a function of the level of normal strain (through the piecewise segmentation of the stress-strain curve). However, in this paper, K^2 is assumed to be a constant.

where

$$\Omega = 2\pi f, \quad \alpha = m\pi/\ell \quad (m=1,2,3,\dots) \quad (15)$$

$f \equiv$ circular frequency of the excitation, and

$$\bar{U} = \frac{q_0(S\alpha)(B'\alpha^2 - R\Omega^2)}{(S\alpha^2 - P\Omega^2)(B'\alpha^2 - R\Omega^2)(B''\alpha^2 - R\Omega^2) - (D\alpha^2 + S - I\Omega^2)(A'\alpha^2 - P\Omega^2) + (S\alpha)^2(A'\alpha^2 - P\Omega^2)} \quad (16)$$

$$\bar{\psi} = \frac{A'\alpha^2 - P\Omega^2}{B'\alpha^2 - R\Omega^2} \bar{U} \quad ; \quad \bar{W} = \frac{1}{S\alpha^2 - P\Omega^2} \left[q_0 - \frac{(S\alpha)(A'\alpha^2 - P\Omega^2)}{B'\alpha^2 - R\Omega^2} \right] \bar{U}$$

Since from equations (7)

$$z_n = -u_{,x}/\psi_{,x} \quad (17)$$

then

$$z_n = \frac{B'\alpha^2 - R\Omega^2}{A'\alpha^2 - P\Omega^2} = \text{constant} \quad (18)$$

4 TRANSFER-MATRIX SOLUTION

The transfer-matrix model used in the present study is the same as that employed in [5] except for the station matrix (see Appendix C), which here includes more terms due to the motion. The transfer matrix for the assumed beam is of the following form

$$[S]_{N_s+1} = [T_f]_{\Delta\ell/2} [T_s] \prod_{i=1}^{N_s-1} ([T_f]_i [T_s]_i) [T_f]_{\Delta\ell/2} [S]_0 \quad (19)$$

where $[T_f]_i$ is the field matrix, $[T_s]_i$ is the station matrix, N_s is the number of stations, $\Delta\ell/2$ is the length of each of the half fields at the ends of the beam, $\Delta\ell$ is the length of each of the whole fields, and $[S]_{N_s+1}$, $[S]_0$ are state vectors, i.e., $(u, w, \psi, N, Q, M)^T$, at the two ends of the beam.

In the calculation of the stiffnesses for the cases where the axial force is not zero, the neutral-surface location and the corresponding distances to the "break points" (a_c and a_t) in the σ_x vs z curve are not constant and not known a-priori. Therefore, an iterative technique has been employed to compute the neutral-surface locations z_n , also a_c and a_t . One must first assume $(2N_s + 2)$

sets of values of z_n , a_c , and a_t and then compute the stiffnesses and solve the governing equations for the state vector. Finally, by using equations (C.1), (C.3), and (C.4), compute the new values of z_n , a_c , and a_t . Obviously, if the assumed and computed sets of z_n , a_c , and a_t are in sufficiently close agreement, the problem is solved; otherwise, assume the calculated set z_n , a_c , and a_t and repeat the procedure.

5 NUMERICAL RESULTS

The numerical results are presented for a thick, multimodular beam with a rectangular cross section. The material of the beam is chosen to be aramid cord-rubber which is used in automobile tires (see Table 1). Four different boundary conditions are investigated (see Table 2) and comparisons are made between multimodular, bimodular, and unimodular models for each set of boundary conditions. In this study, a mesh of twenty-five elements is used with each element being of length of 0.32 in. The shear correction coefficient is taken to be 5/6.

In order to validate the transfer-matrix solution (TMS), Fig. 3, a comparison is made between the closed-form solution (CFS) and the TMS for a guided-guided beam with cosine load distribution (case 1). Also, a comparison is made among unimodular, bimodular, and multimodular (static and dynamic) cases (see also Table 3) for $f = 100$ Hz. As one can see, there is excellent agreement between the TMS and CFS results. However, this agreement can be improved even further by increasing the number of elements.

For the other cases (2-4), the CFS is not available; therefore, in Figs. 4, 6, and 8 comparisons between different models (one, two, and four segment approximations) are made. As one might notice in all four cases, there is considerable difference between transverse deflection of multimodular and bimodular beams on one hand and that of the unimodular model on the other hand. In contrast, there is no substantial difference between multimodular and bimodular results.

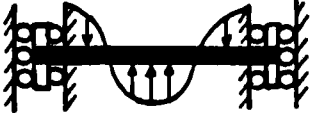
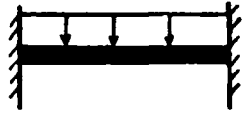
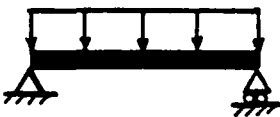

Another interesting observation in Fig. 4 is that for $f = 100$ Hz, the unimodular beam is in the range of its first mode, whereas the bimodular and multi-

Table 1 Elastic properties and geometric parameters for an aramid-cord rubber beam

Elastic Properties	Longitudinal Young's Modulus, MPa (psi x 10 ⁻⁶)				Londitudinal-Thickness Shear Modulus, MPa (psi x 10 ⁻³)	
	Model*	Tension		Compression	Tension and Compression	
	M	E ₂ ^t	E ₁ ^t	E ₁ ^c	E ₂ ^c	G
		4000 (0.580)	2896 (0.420)	221 (0.032)	71 (0.01)	3.70 (0.537)
	B	E _b ^t		E _b ^c		3.70 (0.537)
3240 (0.470)		124 (0.018)				
U	E		E		3.70 (0.537)	
	1896 (0.275)		1896 (0.275)			
Geometric Parameter	Beam length		20.32 cm (8.0 in.)			
	Beam thickness		1.52 cm (0.6 in.)			
	Beam width		2.54 cm (1.0 in.)			

* M ~ multimodular, B ~ bimodular, U ~ unimodular.

Table 2 Summary of cases considered

CASE NO.	BOUNDARY CONDITION AND LOAD POSITION	CASE NO.	BOUNDARY CONDITION AND LOAD POSITION
1		3	
2		4	

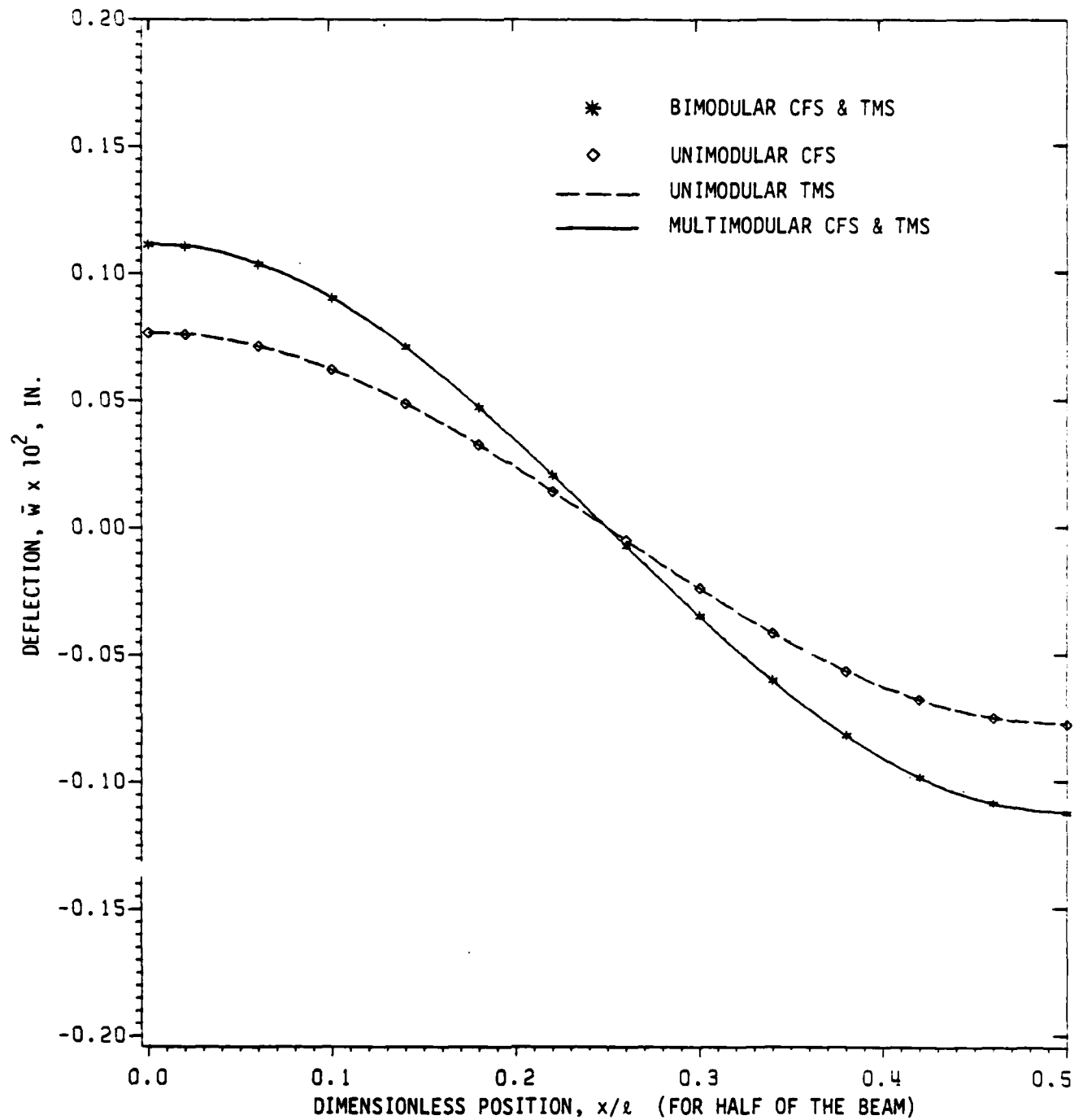


Fig. 3 Comparison among multimodular, bimodular, and unimodular deflection distribution for closed-form and transfer-matrix solutions of guided-guided aramid-cord rubber beam ($f = 100$ Hz)

Table 3 Comparison between CFS* and TMS for an aramid-cord rubber beam (case 1)[†], $f = 100$ Hz

x/ℓ	$\bar{N} \times 10^2, \text{ lb}$		$\bar{Q} \times 10, \text{ lb}$		$\bar{M}, \text{ lb-in.}$	
	CFS	TMS	CFS	TMS	CFS	TMS
0.00	-0.169	-0.164	0.000	0.000	0.203	0.203
0.02	-0.168	-0.162	-0.198	-0.200	0.201	0.202
0.06	-0.157	-0.152	-0.585	-0.587	0.189	0.189
0.10	-0.137	-0.132	-0.935	-0.937	0.164	0.165
0.14	-0.108	-0.104	-1.226	-1.228	0.129	0.130
0.18	-0.072	-0.069	-1.141	-1.143	0.086	0.087
0.22	-0.032	-0.031	-1.565	-1.566	0.038	0.038
0.26	0.011	0.010	-1.590	-1.591	-0.013	-0.013
0.30	0.052	0.050	-1.514	-1.516	-0.063	-0.063
0.34	0.091	0.087	-1.344	-1.346	-0.109	-0.109
0.38	0.123	0.119	-1.089	-1.091	-0.148	-0.148
0.42	0.148	0.143	-0.766	-0.768	-0.178	-0.178
0.46	0.164	0.158	-0.394	-0.396	-0.196	-0.197
0.50	0.169	0.163	0.000	0.000	-0.203	-0.204
0.54	0.164	0.158	0.394	0.396	-0.196	-0.197
0.58	0.148	0.143	0.766	0.768	-0.178	-0.178
0.62	0.123	0.119	1.089	1.091	-0.148	-0.148
0.66	0.091	0.087	1.344	1.346	-0.109	-0.109
0.70	0.052	0.050	1.514	1.516	-0.063	-0.063
0.74	0.011	0.010	1.590	1.591	-0.013	-0.013
0.78	-0.032	-0.031	1.565	1.566	0.038	0.038
0.82	-0.072	-0.069	1.141	1.143	0.086	0.087
0.86	-0.108	-0.104	1.226	1.228	0.129	0.130
0.90	-0.137	-0.132	0.935	0.937	0.164	0.165
0.94	-0.157	-0.152	0.585	0.587	0.189	0.189
0.98	-0.168	-0.162	0.198	0.200	0.201	0.202
1.00	-0.169	-0.164	0.000	0.000	0.203	0.203

* CFS ~ closed-form solution; TMS ~ transfer-matrix solution

[†]For case 1, $Z = z_n/h$ is piecewise constant, equal to $\begin{cases} + 0.3305 & 0 \leq x/\ell < 0.22 \\ - 0.3305 & 0.22 \leq x/\ell < 0.78 \\ + 0.3305 & 0.78 \leq x/\ell \leq 1.00 \end{cases}$

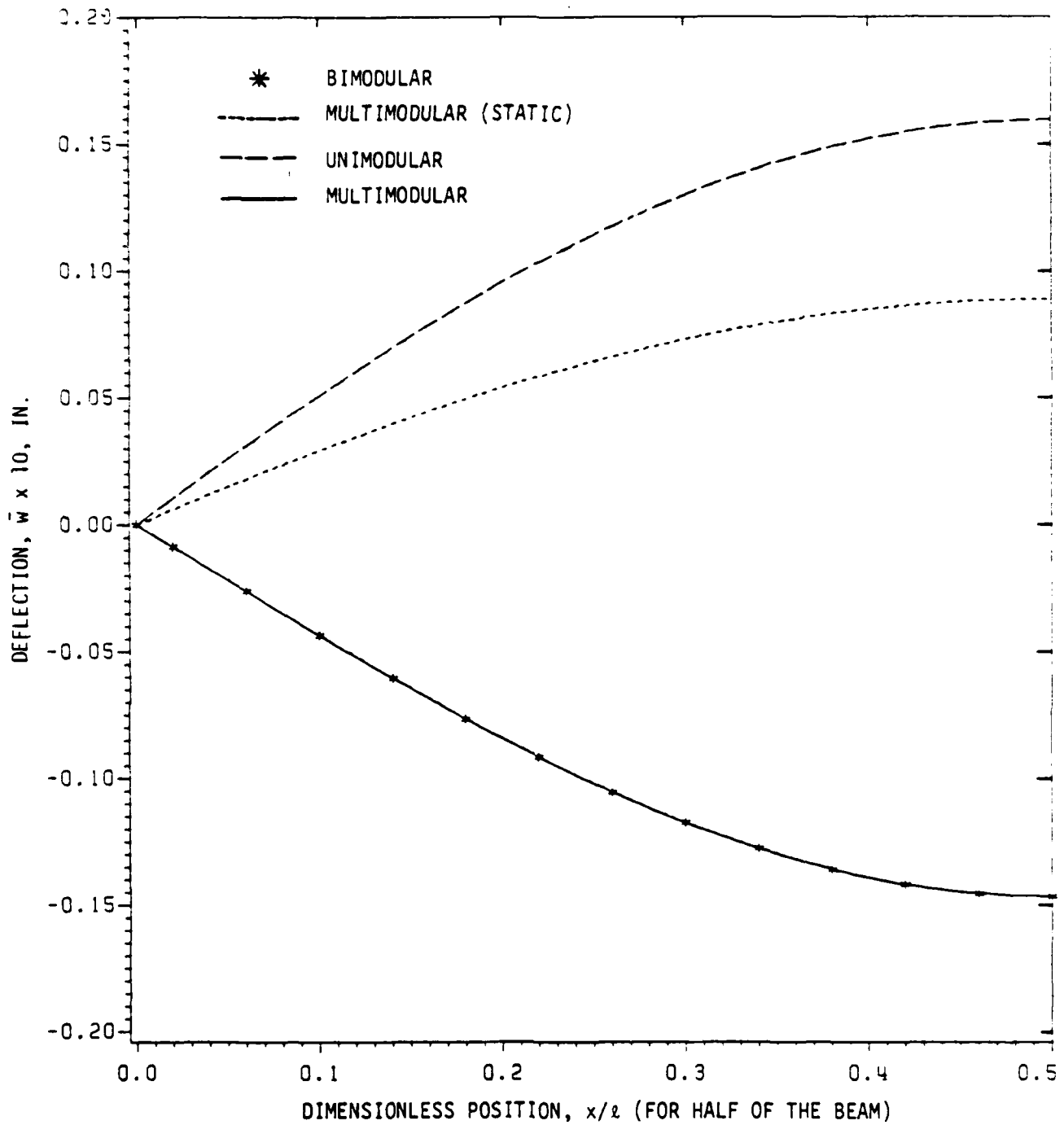


Fig. 4 Comparison among multimodular, bimodular, and unimodular deflection distribution for transfer-matrix solution of hinged-hinged, aramid-cord rubber beam ($f = 100$ Hz)

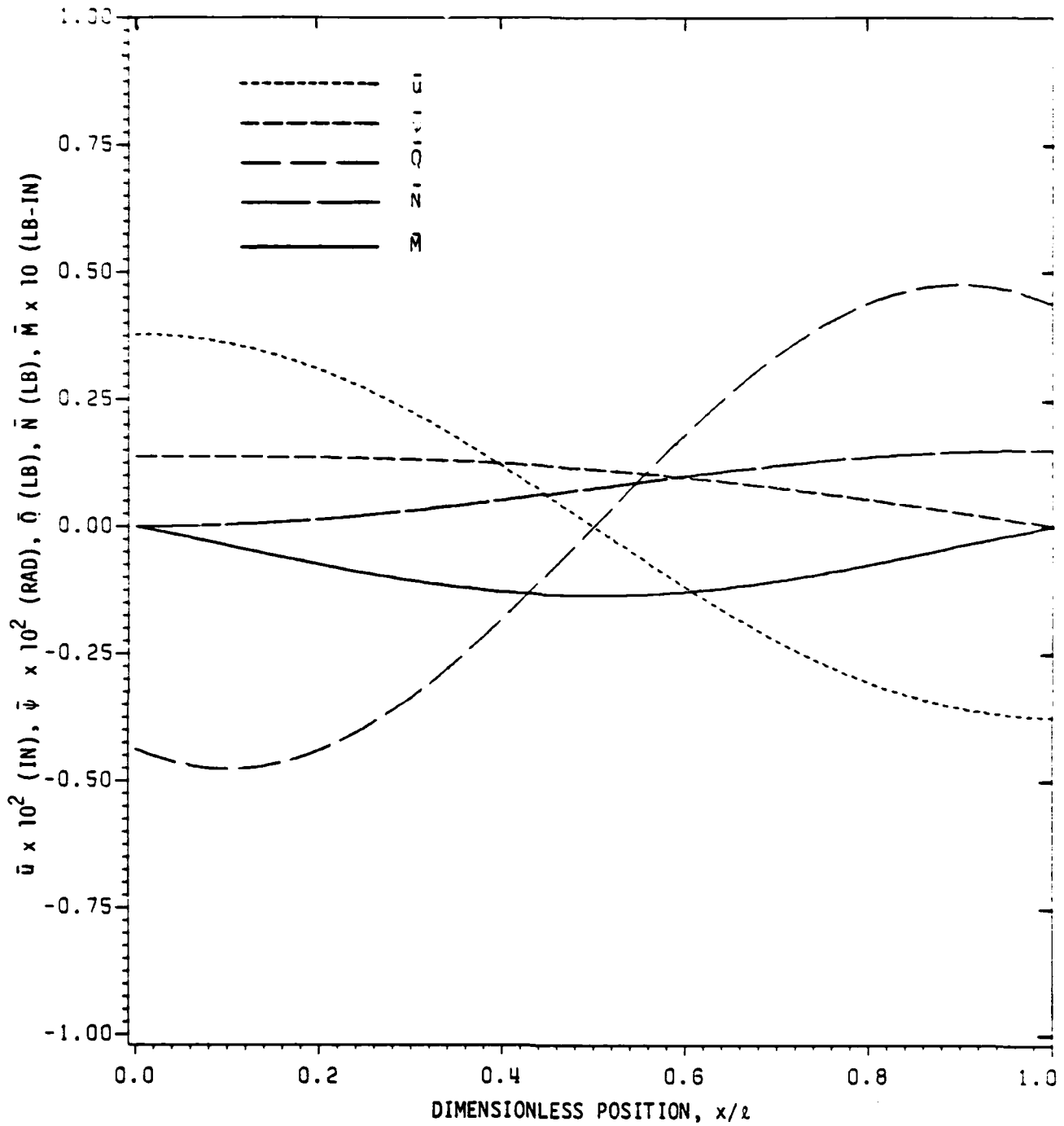


Fig. 5 Transfer-matrix solution of hinged-hinged, aramid-cord rubber beam ($f = 100$ Hz)

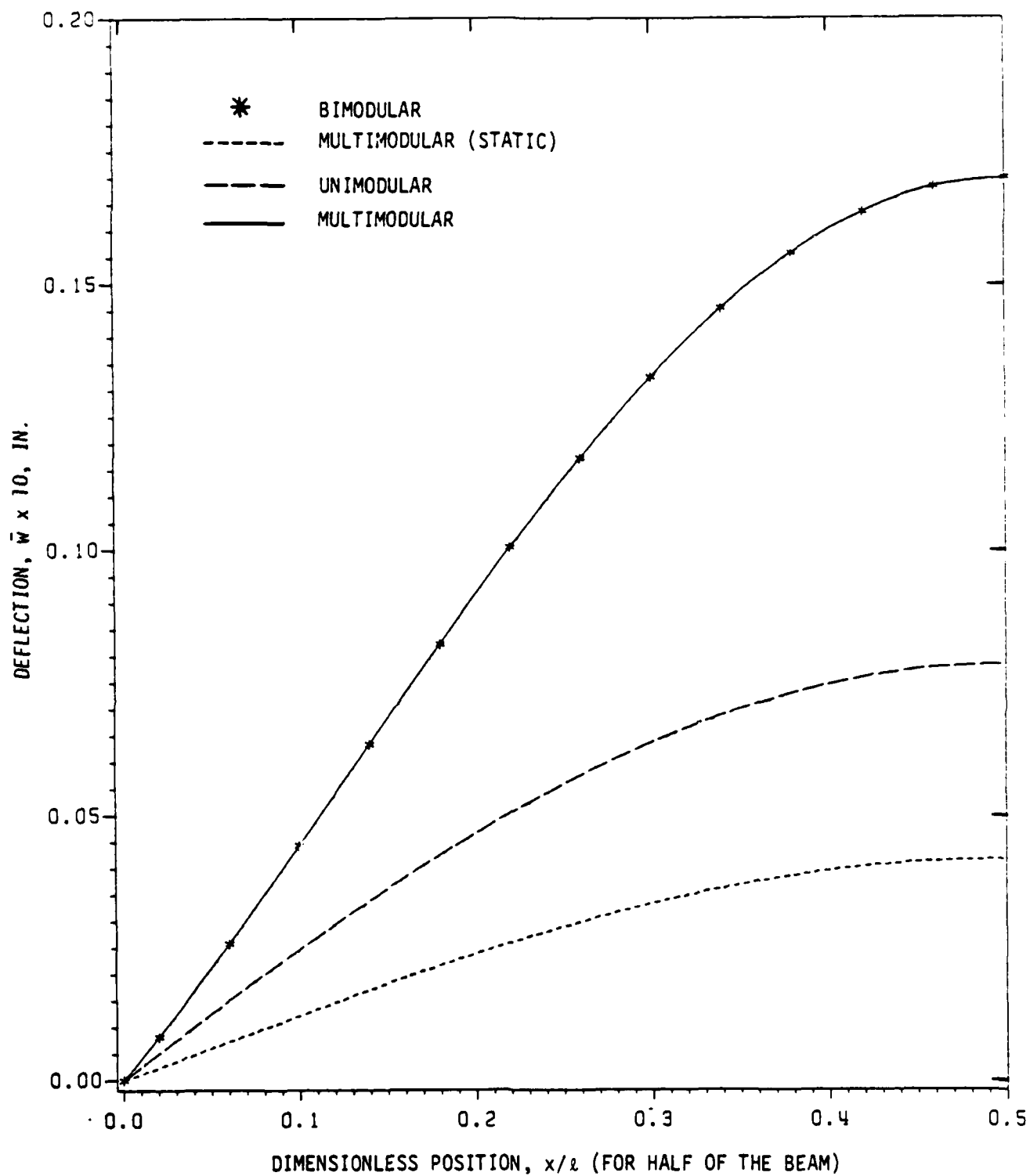


Fig. 6 Comparison among multimodular, bimodular, and unimodular deflection distribution for transfer-matrix solution of clamped-clamped aramid-cord rubber beam ($f = 100$ Hz)

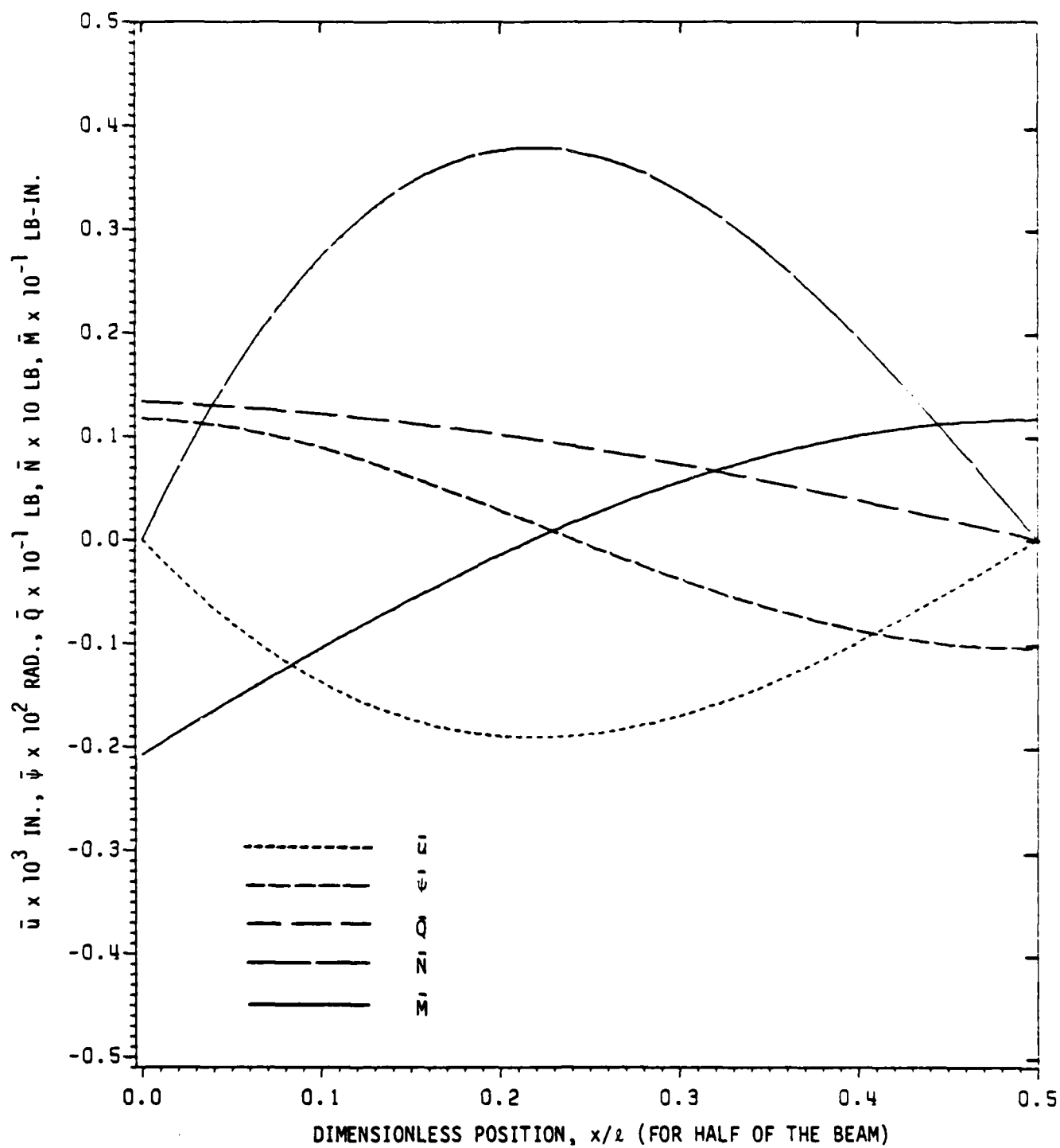


Fig. 7 Transfer-matrix solution of clamped-clamped, aramid-cord rubber beam ($f = 100 \text{ Hz}$)

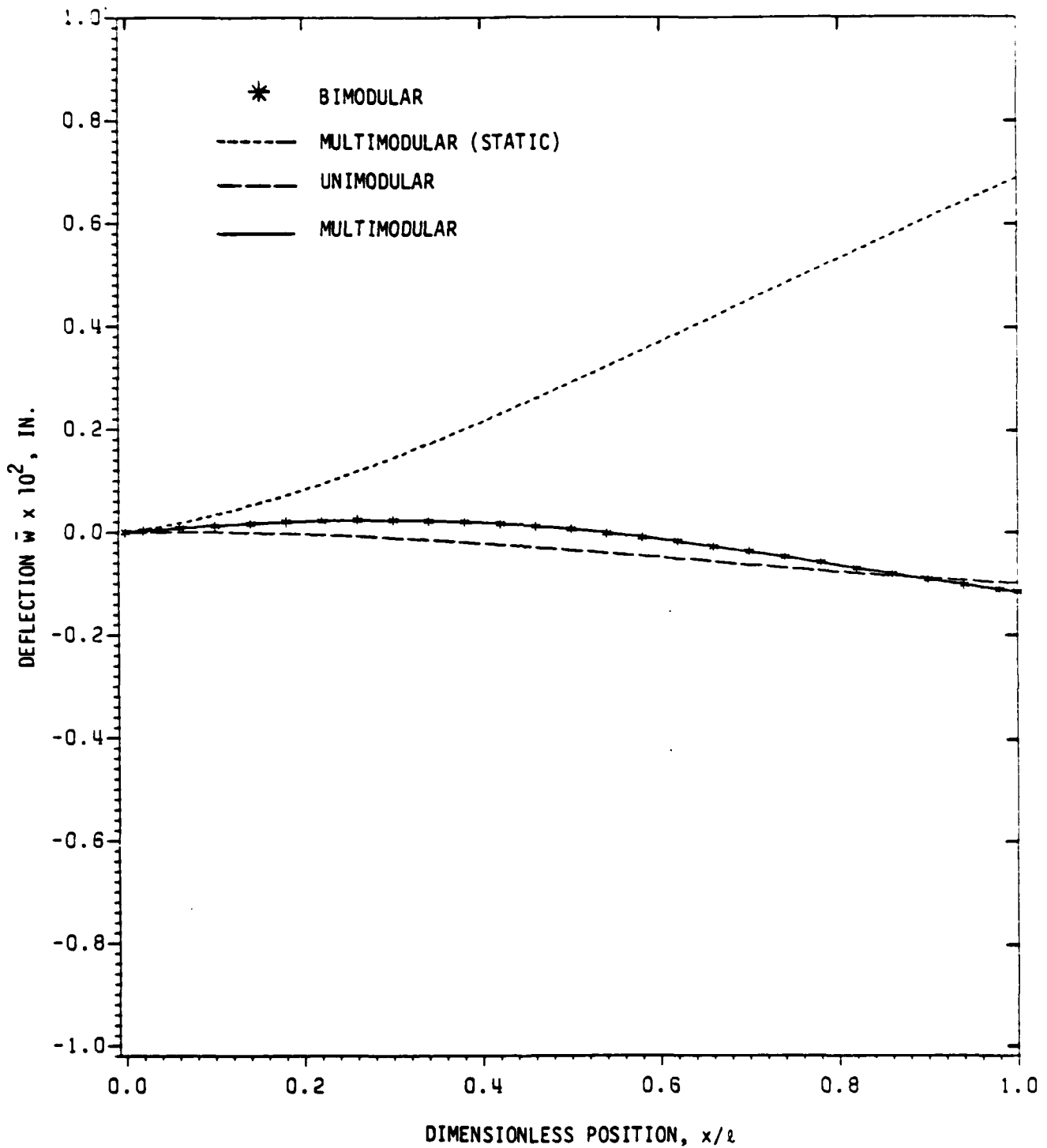


Fig. 8 Comparison among multimodular, bimodular, and unimodular deflection distribution for transfer-matrix solution of clamped-free aramid-cord rubber beam ($f = 100$ Hz)

modular beams are between their first and second modes. The explanation for this is that, for this case (2), most of the layers of the beam are under compression and since E_1^C , E_2^C , and E_b^C are much smaller than E (see Table 1), then the unimodular beam is stiffer than the other two. Therefore, the fundamental frequency of the unimodular beam is higher than those of the bimodular and multimodular beams.

Also, the distributions of \bar{u} (axial displacement), $\bar{\psi}$ (bending slope), \bar{N} (axial force), \bar{Q} (transverse shear force), and \bar{M} (bending moment) are shown graphically in Figures 5, 7, and 9 for f taken to be 100 Hz. Note that for cases 1 and 3 this frequency is less than the fundamental frequency, whereas for cases 2 and 4, the frequency of 100 Hz is in the range of the first and second modes. The first three mode shapes of a clamped-free beam of multimodular material is investigated in Fig. 10. For this case, the natural frequencies associated with the first three modes are $f_1 = 30.9$ Hz, $f_2 = 131.1$ Hz, and $f_3 = 278.5$ Hz.

Finally, by rewriting the equations of motion in a new form ($N_{,x} = P_1 u_{,tt}$, $M_{,x} - Q = I \psi_{,tt}$, $Q_{,x} = P_2 u_{,tt} - q(x,t)$), the effect of translatory and rotatory inertia coefficients on axial force for a thick multimodular clamped-clamped beam ($f = 100$ Hz) is studied (see Table 4). The results show the significant effect of I and slight effect of P_1 as one looks at it through full theory (vibration) as compared to the static case ($I = P_1 = P_2 = 0$).

6 CONCLUSIONS

An analysis of forced vibration of a thick beam with a rectangular cross section and made of "multimodular" material is presented. In this study, numerical results obtained by both the closed-form and transfer-matrix methods are given for a beam made of aramid-cord rubber.

Comparisons are made on one hand between closed-form and transfer-matrix results and on the other hand, among unimodular, bimodular, and multimodular

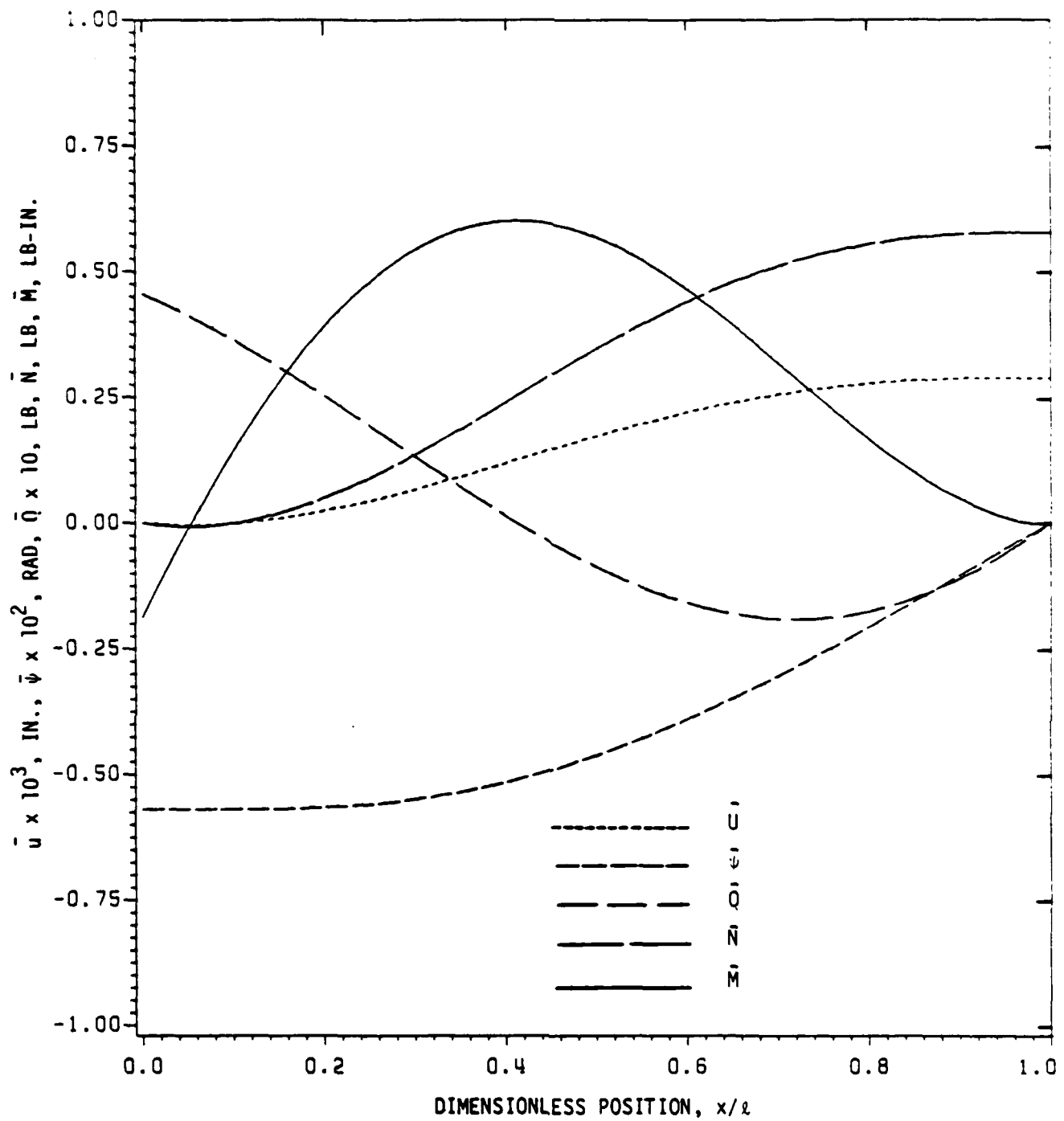


Fig. 9 Transfer-matrix solution of clamped-free aramid-cord rubber beam ($f = 100$ Hz)

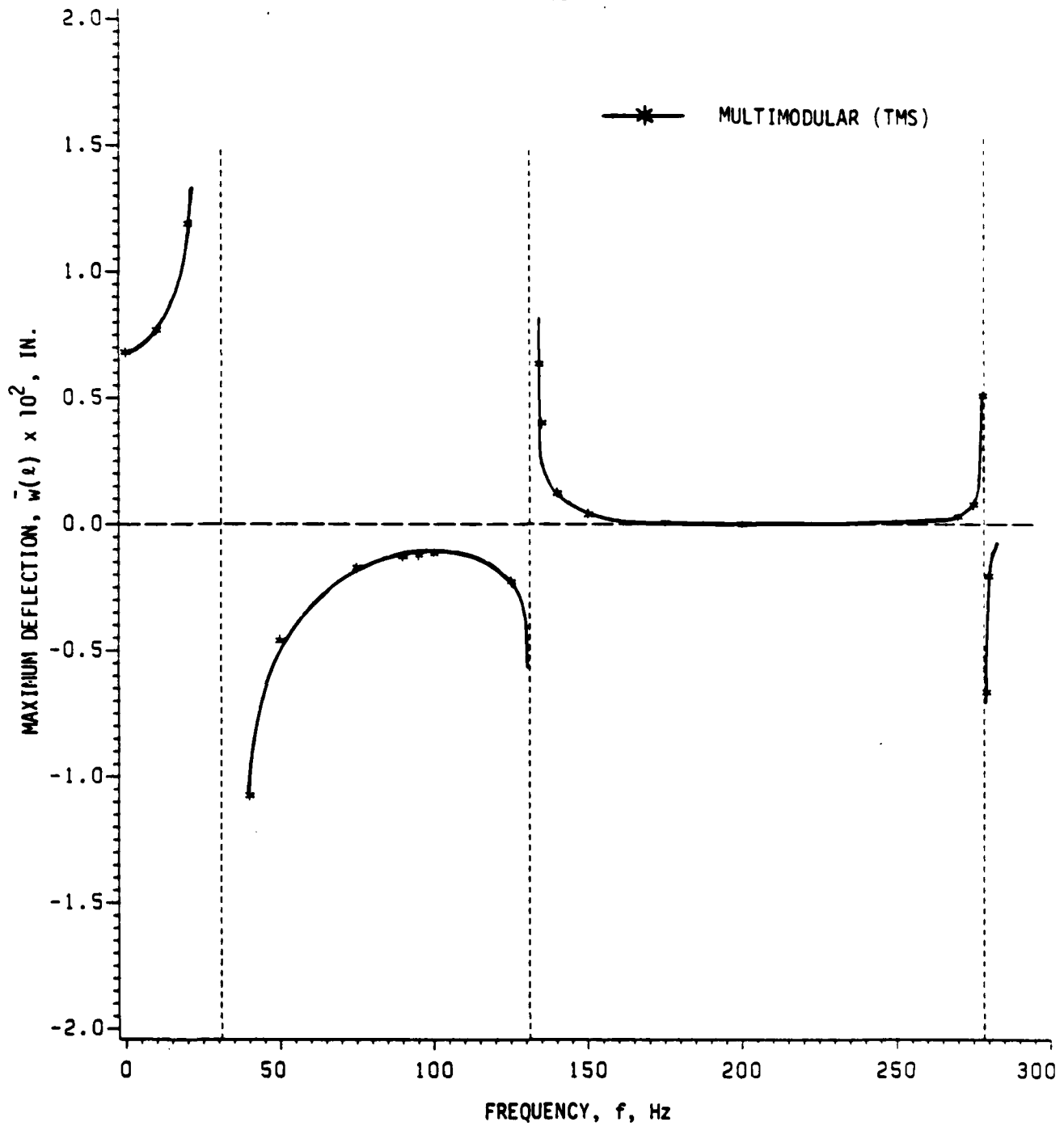


Fig. 10 Investigation of the first three mode shapes of thick multimodular, clamped-free aramid-cord rubber beam with rectangular cross section.

Table 4 Effect of translatory and rotatory inertia coefficients on axial force for a thick multimodular cantilever beam ($f = 100$ Hz)

x/L	Axial force, lb x 10 ³ *				
	I, P ₁ , P ₂ ≠ 0 Full Theory	I=0 P ₁ & P ₂ ≠ 0	I & P ₁ =0 P ₂ ≠ 0	P ₁ =0 I & P ₂ ≠ 0	I, P ₁ , P ₂ =0 Static
0.00	11.74	11.76	-0.1399	-0.1621	-0.0699
0.02	11.49	11.51	-0.1399	-0.1621	-0.0699
0.06	10.56	10.58	-0.1399	-0.1621	-0.0699
0.10	8.90	8.92	-0.1399	-0.1621	-0.0699
0.14	6.69	6.73	-0.1399	-0.1621	-0.0699
0.18	4.15	4.19	-0.1399	-0.1621	-0.0699
0.22	1.44	1.48	-0.1399	-0.1621	-0.0699
0.26	-1.26	-1.21	-0.1399	-0.1621	-0.0699
0.30	-3.82	-3.76	-0.1399	-0.1621	-0.0699
0.34	-6.09	-6.03	-0.1399	-0.1621	-0.0699
0.38	-7.97	-7.91	-0.1399	-0.1621	-0.0699
0.42	-9.38	-9.31	-0.1399	-0.1621	-0.0699
0.46	-10.25	-10.18	-0.1399	-0.1621	-0.0699
0.50	-10.54	-10.47	-0.1399	-0.1621	-0.0699

* 1 lb = 4.448 newtons

models. These results show a considerable difference between the unimodular and bimodular models and a slight difference between the bimodular and multimodular models. Therefore, although a four-segment model is a better approximation, the two-segment approximation gives nearly the same results. This proves that the bimodular model precision is a good approximation.

The values of the first three mode shapes for the clamped-free case are presented. Finally, the effects of axial translatory and rotatory inertia coefficients on axial force for a clamped-clamped beam are discussed.

The transfer-matrix method is found to be very effective in terms of computational time and also in terms of the accuracy of results, which agree very well with the closed-form solution.

References

1. Saint-Venant, B., Notes to the 3rd Ed. of Navier's *Résumé des leçons de la Résistance des corps Solides*, Paris, 1864, p. 175.
2. Timoshenko, S., *Strength of Materials*, Pt. II. Advanced Theory and Problems, 2nd Ed., Van Nostrand, Princeton, NJ, 1941, pp. 362-369.
3. Ambartsumyan, S.A., "The Axisymmetric Problem of a Circular Cylindrical Shell Made of Material with Different Stiffnesses in Tension and Compression", *Izvestiya Akademiiy Nauk SSSR Mekhanika*, No. 4, 1965, pp. 77-84; Engl. Transl., National Tech. Information Center, Document AD-675312, 1967.
4. Tran, A.D. and Bert, C.W., "Bending of Thick Beams of Bimodulus Materials," *Computers and Structures*, Vol. 15, 1982, pp. 627-642.
5. Bert, C.W. and Gordaninejad, F., "Deflection of Thick Beams of Multimodular Materials", *International Journal for Numerical Methods in Engineering*, to appear.
6. Bert, C.W. and Tran, A.D., "Transient Response of a Thick Beam of Bimodular Material", *Earthquake Engineering and Structural Dynamics*, Vol. 10, 1982, pp. 551-560.

7. Pestel, E.C. and Leckie, F.A., *Matrix Methods in Elastomechanics*, Van Nostrand, Princeton, NJ, 1963.
8. Durban, D. and Baruch, M., "Floating Piecewise Linear Approximation of a Nonlinear Constitutive Equation", *AIAA Journal*, Vol. 12, No. 6, June 1974, pp. 868-870.
9. Ramberg, W. and Osgood, W.R., "Description of Stress-Strain Curves by Three Parameters", NACA TN 902, 1943.
10. Bert, C.W. and Kumar, M., "Experimental Investigation of the Mechanical Behavior of Cord-Rubber Materials", Univ. of Oklahoma, Office of Naval Research Contract N00014-78-C-0647, Technical Report No. 23, July 1981.

APPENDIX A: FITTING MINIMIZED CURVES TO THE STRESS-STRAIN CURVE

1. Multimodular Case

Consider the nonlinear stress-strain curve shown in Fig. A.1. For any arbitrary point (ϵ^t, σ^t) in the tension region ($\epsilon \geq 0$), there are two straight lines such that

$$g(\epsilon) \equiv \begin{cases} (\sigma^t/\epsilon^t)\epsilon \\ [(\sigma^t - \sigma_f^t)/(\epsilon^t - \epsilon_f^t)](\epsilon - \epsilon_f^t) + \sigma_f^t \end{cases} \quad (\text{A.1})$$

The equation of a stress-strain curve is

$$\sigma(\epsilon) = K\epsilon^n \quad ; \quad \epsilon \geq 0 \quad (\text{A.2})$$

where K and n are constants depending on the material. To find the proper "break point" (ϵ^t, σ^t) , the area between the approximated curve $g(\epsilon)$ and the actual experimental curve $\sigma(\epsilon)$ has to be minimized. The mentioned area can be expressed

$$A = \left| \int_0^{\epsilon^t} [g_1(\epsilon) - \sigma(\epsilon)] d\epsilon \right| + \left| \int_{\epsilon^t}^{\epsilon_f^t} [g_2(\epsilon) - \sigma(\epsilon)] d\epsilon \right| \quad (\text{A.3})$$

Substitution of equations (A.1) and (A.2) into equation (A.3) and performing the integrations gives

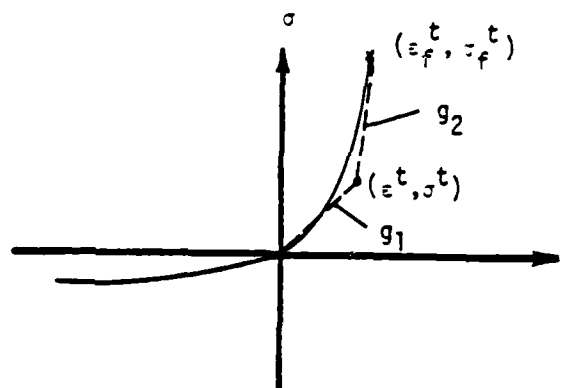


Fig. A.1 Multimodular model.

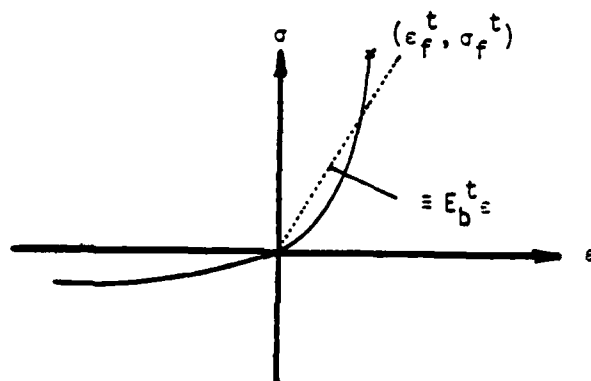


Fig. A.2 Bimodular model.

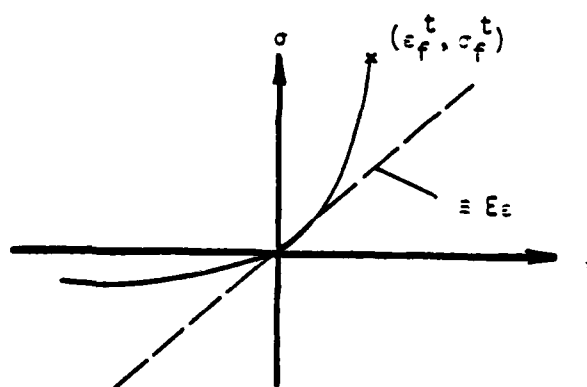


Fig. A.3 Unimodular model.

$$A = \left| \frac{1}{2} \sigma_{\epsilon}^t - \frac{K}{n+1} (\epsilon^t)^{n+1} \right| + \left| \frac{1}{2} (\sigma_f^t + \sigma^t) (\epsilon_f^t - \epsilon^t) - \frac{K}{n+1} [(\epsilon_f^t)^{n+1} - (\epsilon^t)^{n+1}] \right| \quad (A.4)$$

By searching in the region of $\Omega \equiv (0, \epsilon_t^f) \times (0, \sigma_t^f)$, one is able to find a point (ϵ^t, σ^t) such that A is minimized locally. Note that a few other methods (e.g., least-squares method) have been tried but it turned out that the absolute minimum point was outside of the region Ω .

2. Bimodular Case

For this case, the least-squares method has been used. As shown in Fig. A.2, there is a line such that

$$I = \int_0^{\epsilon_f^t} [E_b^t \epsilon - K \epsilon^n]^2 d\epsilon \quad (A.5)$$

can be minimized in Ω . Here, E_b^t is the slope of that line. By taking the derivative of equation (A.5) and equating it to zero, one has

$$\frac{dI}{dE_b^t} = 2 \int_0^{\epsilon_f^t} [E_b^t \epsilon - K \epsilon^n] \epsilon d\epsilon = 0 \quad (A.6)$$

By solving equation (A.6) for E_b^t , one obtains

$$E_b^t = \frac{3K}{n+2} (\epsilon_f^t)^{n-1} \quad (A.7)$$

For example, for aramid-rubber in the tension region, the following parameters are found (the other constants are listed in [10]):

$$n_t = 1.22 \quad ; \quad K_t = 1.1 \times 10^6 \text{ psi} \quad ; \quad \epsilon_f^t = 0.029$$

$$E_b^t = \frac{(3)(1.1 \times 10^6)}{1.22 + 2} (0.029)^{1.22-1} = 0.47 \times 10^6 \text{ psi}$$

An analogous calculation can be applied for the compression side of the bend, i.e., E_b^c can be found, provided that K_c , n_c , and ϵ_f^c are known.

A similar approach can be used to obtain a best-fit single straight line ("unimodular" approximation) [5]; see Fig. A.3.

APPENDIX B: THE BEAM STIFFNESSES FOR RECTANGULAR-SECTION BEAMS OF MULTIMODULAR MATERIALS

For the assumed four-segment model, there are two different bending cases in general, convex downward and concave downward bending. In convex downward bending, the top layer of a beam is in compression and the bottom layer in tension.

A stress distribution for convex downward bending is shown in Fig. 2. As one might notice, the location of z_n , a_c and a_t fall within the depth of the beam (this is case is the most general case). Substitution of equation (1) into equation (8) and using equations (3), (4), and (5) leads to

$$N = \int_{-h/2}^{a_c} [\kappa E_1^c (a_c - z_n) + \kappa E_2^c (z - a_c)] dz + \int_{a_c}^{z_n} \kappa E_1^c (z - z_n) dz + \int_{z_n}^{a_t} \kappa E_1^t (z - z_n) dz + \int_{a_t}^{h/2} [\kappa E_1^t (a_t - z_n) + \kappa E_2^t (z - a_t)] dz \quad (B.1)$$

and

$$M = \int_{-h/2}^{a_c} [\kappa E_1^c (a_c - z_n) + \kappa E_2^c (z - a_c)] z dz + \int_{a_c}^{z_n} \kappa E_1^c (z - z_n) z dz + \int_{z_n}^{a_t} \kappa E_1^t (z - z_n) z dz + \int_{a_t}^{h/2} [\kappa E_1^t (a_t - z_n) + \kappa E_2^t (z - a_t)] z dz \quad (B.2)$$

Equations (B.1) and (B.2) can be written in the following form

$$N = (-\kappa z_n) \left\{ \left[\int_{-h/2}^{a_c} E_2^c dz + \int_{a_c}^{z_n} E_1^c dz + \int_{z_n}^{a_t} E_1^t dz + \int_{a_t}^{h/2} E_2^t dz \right] + \left[- \int_{-h/2}^{a_c} E_2^c dz + \int_{-h/2}^{a_c} E_1^c dz + \int_{a_t}^{h/2} E_1^t dz - \int_{a_t}^{h/2} E_2^t dz \right] \right\}$$

$$\begin{aligned}
& + (\kappa) \left\{ \left[\int_{-h/2}^{a_c} E_2^c z \, dz + \int_{a_c}^{z_n} E_1^c z \, dz + \int_{z_n}^{a_t} E_1^t z \, dz + \int_{a_t}^{h/2} E_2^t z \, dz \right. \right. \\
& \left. \left. + \left[- \int_{-h/2}^{a_c} E_2^c a_c \, dz + \int_{-h/2}^{a_c} E_1^c a_c \, dz + \int_{a_t}^{h/2} E_1^t a_t \, dz - \int_{a_t}^{h/2} E_2^t a_t \, dz \right] \right\} \quad (B.3)
\end{aligned}$$

$$\begin{aligned}
M = (-\kappa z_n) & \left\{ \left[\int_{-h/2}^{a_c} E_2^c z \, dz + \int_{a_c}^{z_n} E_1^c z \, dz + \int_{z_n}^{a_t} E_1^t z \, dz + \int_{a_t}^{h/2} E_2^t z \, dz \right] \right. \\
& + \left[- \int_{-h/2}^{a_c} E_2^c z \, dz + \int_{-h/2}^{a_c} E_1^c z \, dz + \int_{a_t}^{h/2} E_1^t z \, dz - \int_{a_t}^{h/2} E_2^t z \, dz \right] \\
& + (\kappa) \left\{ \left[\int_{-h/2}^{a_c} E_2^c z^2 \, dz + \int_{a_c}^{z_n} E_1^c z^2 \, dz + \int_{z_n}^{a_t} E_1^t z^2 \, dz + \int_{a_t}^{h/2} E_2^t z^2 \, dz \right] \right. \\
& \left. + \left[- \int_{-h/2}^{a_c} E_2^c a_c \, dz + \int_{-h/2}^{a_c} E_1^c a_c \, dz + \int_{a_t}^{h/2} E_1^t a_t \, dz - \int_{a_t}^{h/2} E_2^t a_t \, dz \right] \right\} \quad (B.4)
\end{aligned}$$

Combining equations (7) and (9), one gets

$$N = (-\kappa z_n) A' + \kappa B' \quad (B.5)$$

$$M = (-\kappa z_n) B'' + \kappa D' \quad (B.6)$$

Comparison of equations (B.3) and (B.5) with equations (B.4) and (B.6) and considering equations (10), one finds that

$$\begin{aligned}
C_A^N &= \int_{-h/2}^{a_c} (E_1^c - E_2^c) \, dz + \int_{a_t}^{h/2} (E_1^t - E_2^t) \, dz \\
C_B^N &= \int_{-h/2}^{a_c} (E_1^c - E_2^c) a_c \, dz + \int_{a_t}^{h/2} (E_1^t - E_2^t) a_t \, dz
\end{aligned}$$

$$\begin{aligned}
C_B^M &= \int_{-h/2}^{a_c} (E_1^c - E_2^c) z \, dz + \int_{a_c}^{h/2} (E_1^t - E_2^t) z \, dz \\
C_D^M &= \int_{-h/2}^{a_c} (E_1^c - E_2^c) a_c z \, dz + \int_{a_t}^{h/2} (E_1^t - E_2^t) a_t z \, dz
\end{aligned} \tag{B.7}$$

Eight possible cases may occur depending on the location of z_n , a_c , and a_t . These cases have been analyzed as the same as the general case as follows (for convex downward bending).

There are seven more possible cases which have been discussed in Ref. [5]. However, the case explained here is the most general case.

APPENDIX C: TRANSFER-MATRIX FORMULATION

Under harmonic excitation, the steady-state-response displacements u , w , and ψ are also harmonic in time. Therefore, equations (11) can be written as

$$\begin{aligned}
\bar{N}_{,x} &= -\Omega^2 P \bar{u} - \Omega^2 R \bar{\psi} \quad ; \quad \bar{Q}_{,x} = -\Omega^2 P \bar{w} - q(x,t) \\
\bar{M}_{,x} - \bar{Q} &= -\Omega^2 R \bar{u} - \Omega^2 I \bar{\psi}
\end{aligned} \tag{C.1}$$

where all of the barred quantities are amplitudes, i.e., $N(x,t) = \bar{N}(x) \sin \Omega t$, etc. The continuity at each station implies

$$\bar{u}_i^R = \bar{u}_i^L \quad , \quad \bar{w}_i^R = \bar{w}_i^L \quad , \quad \bar{\psi}_i^R = \bar{\psi}_i^L \tag{C.2}$$

(R and L denote right and left, respectively)

Also, equation (C.1) in finite-differential form for each station i is

$$\begin{aligned}
\bar{N}_i^R &= \bar{N}_i^L - \Omega^2 P \bar{u}_i^L \quad ; \quad \bar{Q}_i^R = \bar{Q}_i^L - \Omega^2 P \bar{w}_i^L - \bar{Q}_i \\
\bar{M}_i^R &= \bar{M}_i^L - \Omega^2 R \bar{u}_i^L - \Omega^2 I \bar{\psi}_i^L
\end{aligned} \tag{C.3}$$

where Q_i is the concentrated load amplitude at station i .

Equations (A.2) and (A.3) are written in matrix notation as

$$\left\{ \begin{array}{c} \bar{u} \\ \bar{w} \\ \bar{\psi} \\ \bar{N} \\ \bar{Q} \\ \bar{M} \\ 1 \end{array} \right\}_i^R = \left[\begin{array}{cccccc} 1 & 0 & 0 & 0 & 0 & 0 \\ 0 & 1 & 0 & 0 & 0 & 0 \\ 0 & 0 & 1 & 0 & 0 & 0 \\ -\Omega^2 P & 0 & -\Omega^2 R & 1 & 0 & 0 \\ 0 & -\Omega^2 P & 0 & 0 & 1 & 0 \\ -\Omega^2 R & 0 & -\Omega^2 I & 0 & 0 & 1 \\ 0 & 0 & 0 & 0 & 0 & 1 \end{array} \right]_i \left\{ \begin{array}{c} \bar{u} \\ \bar{w} \\ \bar{\psi} \\ \bar{N} \\ \bar{Q} \\ \bar{M} \\ 1 \end{array} \right\}_i^L \quad (C.4)$$

or

$$[S]_i^R = [T_S]_i [S]_i^L$$

where $[T_S]_i$ represents station matrix at station i . In matrix notation the equilibrium equation for each field under a distributed load $q(x)$ is

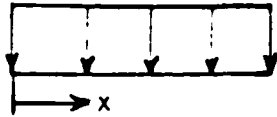
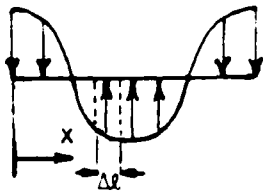
$$\left\{ \begin{array}{c} u \\ w \\ \psi \\ N \\ Q \\ M \\ 1 \end{array} \right\}_{i+1} = \left[\begin{array}{cccccc} 1 & 0 & 0 & \frac{B' \Delta \ell}{\gamma} & \frac{B' (\Delta \ell)^2}{2\gamma} & \frac{-D' \Delta \ell}{\gamma} & \frac{-B' \Delta \ell}{2\gamma} K_m \\ 0 & 1 & -\Delta \ell & \frac{A' (\Delta \ell)^2}{2\gamma} & \left[\frac{\Delta \ell}{5} + \frac{A' (\Delta \ell)^3}{4\gamma} \right] & \frac{-B' (\Delta \ell)^2}{2\gamma} & \frac{-A' (\Delta \ell)^2}{4\gamma} K_m - \frac{\Delta \ell}{2S} K_q \\ 0 & 0 & 1 & \frac{-A' \Delta \ell}{\gamma} & \frac{-A' (\Delta \ell)^2}{2\gamma} & \frac{B' \Delta \ell}{\gamma} & \frac{A' \Delta \ell}{2\gamma} K_m \\ 0 & 0 & 0 & 1 & 0 & 0 & 0 \\ 0 & 0 & 0 & 0 & 1 & 0 & -K_q \\ 0 & 0 & 0 & 0 & \Delta \ell & 1 & -K_m \\ 0 & 0 & 0 & 0 & 0 & 0 & 1 \end{array} \right]_i \left\{ \begin{array}{c} u \\ w \\ \psi \\ N \\ Q \\ M \\ 1 \end{array} \right\}_i \quad (C.5)$$

where

$$\gamma \equiv B'B'' - A'D' \quad ; \quad K_q \equiv \int_0^{\Delta \ell} q(\xi) d\xi \quad ; \quad K_m \equiv \int_0^{\Delta \ell} \xi q(\xi) d\xi \quad (C.6)$$

Values of K_m and K_q for various loadings are listed in Table 5. Equation (C.6) also can be written as

Table 5 Values of K_m and K_q for various loadings

Type of Loading	K_m	K_q
Uniform Load $q(x) = q_0$ 	$q_0 (\Delta l)^2 / 2$	$q_0 \Delta l$
Cosine Load $q(x) = q_0 \cos \frac{n\pi}{l} x$ 	$\frac{q_0 l}{n\pi} \left[-\frac{l}{n\pi} \left(\cos \frac{n\pi}{l} x_j - \cos \frac{n\pi}{l} x_{j-1} \right) - l \sin \frac{n\pi}{l} x_{j-1} \right]$	$\frac{q_0 l}{n\pi} \left(\sin \frac{n\pi}{l} x_j - \sin \frac{n\pi}{l} x_{j-1} \right)$

$$[S]_{i+1}^L = [T_j]_i [S]_i^R \quad (C.7)$$

The matrix $[T_j]_i$ is called the field matrix.

APPENDIX D: COMPUTATION OF z_n , a_c , AND a_t

For multimodular beams, the following equation is not sufficient to determine the neutral-surface location z_n

$$z_n = \frac{B'M - D'N}{A'M - B''N} \quad (D.1)$$

even for cases where $N = 0$

$$z_n = B'/A' \quad (D.2)$$

Two more equations are needed for computing z_n because the stiffnesses are not only dependent on z_n but they are functions of a_c and a_t as well. By comparison of Figures 1 and 2, one can get (for the convex downward case)

$$a_c = (\epsilon_1^c / \epsilon_f^c) (h/2 + z_n) - z_n \quad (D.3)$$

$$a_t = (\epsilon_1^t / \epsilon_f^t) (h/2 - z_n) + z_n \quad (D.4)$$

For the concave downward case

$$a_c = (\epsilon_1^c / \epsilon_f^c) (h/2 - z_n) + z_n \quad (D.5)$$

$$a_t = (\epsilon_1^t / \epsilon_f^t) (h/2 + z_n) - z_n \quad (D.6)$$

The system of nonlinear equations (D.1), (D.3), and (D.4) for the convex downward case, or equations (D.1), (D.5), and (D.6) for the concave downward case, can be solved by using iteration of the Gauss-Seidel type.

PREVIOUS REPORTS ON THIS CONTRACT

Project Rept. No.	Issuing University Rept. No.*	Report Title	Author(s)
1	OU 79-7	Mathematical Modeling and Micromechanics of Fiber Reinforced Bimodulus Composite Material	C.W. Bert
2	OU 79-8	Analyses of Plates Constructed of Fiber-Reinforced Bimodulus Materials	J.N. Reddy & C.W. Bert
3	OU 79-9	Finite-Element Analyses of Laminated Composite-Material Plates	J.N. Reddy
4A	OU 79-10A	Analyses of laminated Bimodulus Composite-Material Plates	C.W. Bert
5	OU 79-11	Recent Research in Composite and Sandwich Plate Dynamics	C.W. Bert
6	OU 79-14	A Penalty Plate-Bending Element for the Analysis of Laminated Anisotropic Composite Plates	J.N. Reddy
7	OU 79-18	Finite-Element Analysis of Laminated Bimodulus Composite-Material Plates	J.N. Reddy & W.C. Chao
8	OU 79-19	A Comparison of Closed-Form and Finite-Element Solutions of Thick Laminated Anisotropic Rectangular Plates	J.N. Reddy
9	OU 79-20	Effects of Shear Deformation and Anisotropy on the Thermal Bending of Layered Composite Plates	J.N. Reddy & Y.S. Hsu
10	OU 80-1	Analyses of Cross-Ply Rectangular Plates of Bimodulus Composite Material	V.S. Reddy & C.W. Bert
11	OU 80-2	Analysis of Thick Rectangular Plates Laminated of Bimodulus Composite Materials	C.W. Bert, J.N. Reddy, V.S. Reddy, & W.C. Chao
12	OU 80-3	Cylindrical Shells of Bimodulus Composite Material	C.W. Bert & V.S. Reddy
13	OU 80-6	Vibration of Composite Structures	C.W. Bert
14	OU 80-7	Large Deflection and Large-Amplitude Free Vibrations of Laminated Composite-Material Plates	J.N. Reddy & W.C. Chao
15	OU 80-8	Vibration of Thick Rectangular Plates of Bimodulus Composite Material	C.W. Bert, J.N. Reddy, W.C. Chao, & V.S. Reddy
16	OU 80-9	Thermal Bending of Thick Rectangular Plates of Bimodulus Material	J.N. Reddy, C.W. Bert, Y.S. Hsu, & V.S. Reddy
17	OU 80-14	Thermoelasticity of Circular Cylindrical Shells Laminated of Bimodulus Composite Materials	Y.S. Hsu, J.N. Reddy, & C.W. Bert
18	OU 80-17	Composite Materials: A Survey of the Damping Capacity of Fiber-Reinforced Composites	C.W. Bert
19	OU 80-20	Vibration of Cylindrical Shells of Bimodulus Composite Materials	C.W. Bert & M. Kumar
20	VPI 81-11 & OU 81-1	On the Behavior of Plates Laminated of Bimodulus Composite Materials	J.N. Reddy & C.W. Bert
21	VPI 81-12	Analysis of Layered Composite Plates Accounting for Large Deflections and Transverse Shear Strains	J.N. Reddy
22	OU 81-7	Static and Dynamic Analyses of Thick Beams of Bimodular Materials	C.W. Bert & A.D. Tran
23	OU 81-8	Experimental Investigation of the Mechanical Behavior of Cord-Rubber Materials	C.W. Bert & M. Kumar
24	VPI 81.28	Transient Response of Laminated, Bimodular-Material Composite Rectangular Plates	J.N. Reddy
25	VPI 82.2	Nonlinear Bending of Bimodular-Material Plates	J.N. Reddy & W.C. Chao
26	OU 82-2	Analytical and Experimental Investigations of Bimodular Composite Beams	C.W. Bert, C.A. Rebello, & C.J. Rebello
27	OU 82-3	Research on Dynamics of Composite and Sandwich Plates, 1979-81	C.W. Bert
28	OU 82-4 & VPI 82.20	Mechanics of Bimodular Composite Structures	C.W. Bert & J.N. Reddy

*OU denotes the University of Oklahoma; VPI denotes Virginia Polytechnic Institute and State University.

Previous Reports on this Contract - Cont'd
Page 2

<u>Project Rept. No.</u>	<u>Issuing University Rept. No.</u>	<u>Report Title</u>	<u>Author(s)</u>
29	VPI 82.19	Three-Dimensional Finite Element Analysis of Layered Composite Structures	W.C. Chao, N.S. Putcha, J.N. Reddy
30	OU 82-5	Analyses of Beams Constructed of Nonlinear Materials Having Different Behavior in Tension and Compression	C.W. Bert & F. Gordaninejad
31	VPI 82.31	Analysis of Layered Composite Plates by Three-Dimensional Elasticity Theory	J.N. Reddy & T. Kuppusamy
32	OU 83-1	Transverse Shear Effects in Bimodular Composite Laminates	C.W. Bert & F. Gordaninejad

UNCLASSIFIED

SECURITY CLASSIFICATION OF THIS PAGE (When Data Entered)

REPORT DOCUMENTATION PAGE		READ INSTRUCTIONS BEFORE COMPLETING FORM
1. REPORT NUMBER OU-AMNE-83-2	2. GOVT ACCESSION NO. ADA130372	3. RECIPIENT'S CATALOG NUMBER
4. TITLE (and Subtitle) FORCED VIBRATION OF TIMOSHENKO BEAMS MADE OF MULTIMODULAR MATERIALS	5. TYPE OF REPORT & PERIOD COVERED Technical Report No. 33	
7. AUTHOR(s) F. Gordaninejad and C.W. Bert	6. PERFORMING ORG. REPORT NUMBER	
9. PERFORMING ORGANIZATION NAME AND ADDRESS School of Aerospace, Mechanical and Nuclear Engineering University of Oklahoma, Norman, OK 73019	8. CONTRACT OR GRANT NUMBER(s) N00014-78-C-0647	
11. CONTROLLING OFFICE NAME AND ADDRESS Department of the Navy, Office of Naval Research Mechanics Division (Code 432) Arlington, Virginia 22217	10. PROGRAM ELEMENT, PROJECT, TASK AREA & WORK UNIT NUMBERS NR 064-609	
14. MONITORING AGENCY NAME & ADDRESS (if different from Controlling Office)	12. REPORT DATE June 1983	
	13. NUMBER OF PAGES 31	
	15. SECURITY CLASS. (of this report) UNCLASSIFIED	
	15a. DECLASSIFICATION/DOWNGRADING SCHEDULE	
16. DISTRIBUTION STATEMENT (of this Report) This document has been approved for public release and sale; distribution unlimited.		
17. DISTRIBUTION STATEMENT (of the abstract entered in Block 20, if different from Report)		
18. SUPPLEMENTARY NOTES This paper is to be presented at the 19th ASME Conference on Mechanical Vibration and Noise, Dearborn, MI, Sept. 12-14, 1983.		
19. KEY WORDS (Continue on reverse side if necessary and identify by block number) Beams, bending theory, bending-stretching coupling, bimodular materials, multimodular materials, nonlinear materials, Timoshenko beam theory, transfer-matrix method, vibration.		
20. ABSTRACT (Continue on reverse side if necessary and identify by block number) → This paper presents a transfer-matrix analysis for determining the sinusoidal vibration response of thick, rectangular-cross-section beams made of "multimodular materials" (i.e., materials which have different elastic behavior in tension and compression, with nonlinear stress-strain curves approximated as piecewise linear). An experimentally determined stress-strain curve for aramid-cord rubber is approximated by four straight-line segments (two segments in tension and two segments in compression). To validate (over)		

DD FORM 1473
1 JAN 73EDITION OF 1 NOV 68 IS OBSOLETE
S/N 0102-014-6601UNCLASSIFIED
SECURITY CLASSIFICATION OF THIS PAGE (When Data Entered)

UNCLASSIFIED

SECURITY CLASSIFICATION OF THIS PAGE(When Data Entered)

20. Abstract - Cont'd

the transfer-matrix results, a closed-form solution is also presented for the special case in which the neutral-surface location is uniform along the length of the beam. Also, comparisons are made among multimodular, bimodular (two line segments), and unimodular models. Numerical results for axial displacement, transverse deflection, bending slope, bending moment, transverse shear and axial forces, and the location of the neutral surface are presented for the multimodular model. Effects of translatory and rotatory inertia coefficients on axial force are investigated for a clamped-clamped beam. Moreover, natural frequencies associated with the first three modes of a clamped-free beam are presented. Transfer-matrix results agree very well with the closed-form results for the corresponding material model (one, two, or four segments).

UNCLASSIFIED

SECURITY CLASSIFICATION OF THIS PAGE(When Data Entered)

DATE
ILME